

PAPER • OPEN ACCESS

Sub-gap optical response in the Kitaev spin-liquid candidate α -RuCl₃

To cite this article: Stephan Reschke *et al* 2018 *J. Phys.: Condens. Matter* **30** 475604

View the [article online](#) for updates and enhancements.



IOP | ebooks™

Bringing you innovative digital publishing with leading voices to create your essential collection of books in STEM research.

Start exploring the collection - download the first chapter of every title for free.

Sub-gap optical response in the Kitaev spin-liquid candidate α -RuCl₃

Stephan Reschke¹, Franz Mayr¹, Sebastian Widmann¹,
Hans-Albrecht Krug von Nidda¹, Vladimir Tsurkan^{1,2}, Mikhail V Eremin³,
Seung-Hwan Do⁴, Kwang-Yong Choi⁴, Zhe Wang⁵ and Alois Loidl^{1,6}

¹ Experimental Physics V, Center for Electronic Correlations and Magnetism, University of Augsburg, 86135 Augsburg, Germany

² Institute of Applied Physics, MD 2028 Chisinau, Moldova

³ Kazan Federal (Volga region) University, 420008, Russia

⁴ Department of Physics, Chung-Ang University, Seoul 06974, Republic of Korea

⁵ Institute of Radiation Physics, Helmholtz-Zentrum Dresden-Rossendorf, 01328 Dresden, Germany

E-mail: alois.loidl@physik.uni-augsburg.de

Received 9 July 2018, revised 3 October 2018

Accepted for publication 12 October 2018


Published 5 November 2018



Abstract

We report detailed optical experiments on the layered compound α -RuCl₃ focusing on the THz and sub-gap optical response across the structural phase transition from the monoclinic high-temperature to the rhombohedral low-temperature structure, where the stacking sequence of the molecular layers is changed. This type of phase transition is characteristic for a variety of tri-halides crystallizing in a layered honeycomb-type structure and so far is unique, as the low-temperature phase exhibits the higher symmetry. One motivation is to unravel the microscopic nature of THz and spin-orbital excitations via a study of temperature and symmetry-induced changes. The optical studies are complemented by thermal expansion experiments. We document a number of highly unusual findings: A characteristic two-step hysteresis of the structural phase transition, accompanied by a dramatic change of the reflectivity. A complex dielectric loss spectrum in the THz regime, which could indicate remnants of Kitaev physics. Orbital excitations, which cannot be explained based on recent models, and an electronic excitation, which appears in a narrow temperature range just across the structural phase transition. Despite significant symmetry changes across the monoclinic to rhombohedral phase transition and a change of the stacking sequence, phonon eigenfrequencies and the majority of spin-orbital excitations are not strongly influenced. Obviously, the symmetry of a single molecular layer determines the eigenfrequencies of most of these excitations. Only one mode at THz frequencies, which becomes suppressed in the high-temperature monoclinic phase and one phonon mode experience changes in symmetry and stacking. Finally, from this combined terahertz, far- and mid-infrared study we try to shed some light on the so far unsolved low energy (<1 eV) electronic structure of the ruthenium 4d⁵ electrons in α -RuCl₃.

⁶ Author to whom any correspondence should be addressed.

 Original content from this work may be used under the terms of the [Creative Commons Attribution 3.0 licence](https://creativecommons.org/licenses/by/3.0/). Any further distribution of this work must maintain attribution to the author(s) and the title of the work, journal citation and DOI.

Keywords: α -RuCl₃, Kitaev spin liquids, dielectric and optical properties, THz, FIR and MIR spectroscopy, phonons, orbital excitations, structural phase transition

 Supplementary materials for this article is available [online](#)

(Some figures may appear in colour only in the online journal)

1. Introduction

After early reports on synthesis and structure of α -RuCl₃ [1], Fletcher *et al* [2, 3] reported on synthesis as well as on structural, magnetic, and optical characterization. The structural units of α -RuCl₃ are honeycomb layers of ruthenium, separated by two hexagonal layers of chlorine. Ru³⁺ ($4d^5$) is coordinated by Cl⁻ ions in octahedral symmetry with slight monoclinic distortion. The ruthenium layers, sandwiched between two layers of chlorine, represent strongly bonded molecular stacks, only weakly connected by van der Waals (vdW) forces. Due to the weak vdW binding energy between the molecular stacks, the structure is prone to stacking faults. Early structural studies reported on a highly symmetric $P3_112$ space group [1–3]. However, now it seems well established that the room temperature symmetry of α -RuCl₃ is monoclinic with space group $C2/m$ [4–6], isostructural to the infinite-layer compound CrCl₃ at 300 K [7]. As observed in a number of layered tri-halides [7–9], also α -RuCl₃ undergoes a transition into a low-temperature rhombohedral structure with $R\bar{3}$ symmetry. This transition is located around 150 K [10–15] and is characterized by a wide hysteresis. A similar phase transition, induced by changes of the molecular stacking sequence, also appears in chromium tri-chloride at 240 K [7, 9], in chromium tri-iodide close to 220 K [8], in chromium tri-bromide at approximately 420 K [7], and in ScCl₃ at \sim 950 K [16]. In the low-temperature structure, the halide ions are hexagonal close-packed, with an AB-type stacking sequence, in contrast to the face-centred cubic ABC stacking of the high-temperature monoclinic form [7]. This monoclinic-to-rhombohedral transition can occur by a simple translational shift of neighbouring layers along one direction [7]. The structural phase transition involving a shift of neighbouring 2D building blocks by itself is an interesting phenomenon: Recently it has been shown that the twist angle between neighbouring graphene layers plays a crucial role in the electronic properties [17] and can even induce superconductivity at certain twist angles [18]. In addition, all tri-halides are vdW layered materials showing unconventional phase transitions similar to experimental findings in transition-metal dichalcogenides [19].

Here it should be mentioned that during the last years different structures of α -RuCl₃ have been reported. In a detailed structural study by Johnson *et al* [20] on detwinned single crystals, the authors were able to exclude a low-temperature rhombohedral phase with a three-layer stacking sequence in their crystals. At 80 K these authors identified a monoclinic phase with a number stacking faults. These crystals are characterized by a single and well-defined magnetic phase

transition at 13 K [20]. Ziatdinov *et al* [21] report on a structural phase transition at \sim 150 K with a width of \sim 30 K from a low-temperature monoclinic structure to a $P3_1$ type stacking order. In the last two years, scientific reports converge to a low-temperature rhombohedral phase with a magnetic order close to 7 K and with a low density of stacking faults [22, 23].

Quite recently, α -RuCl₃ characterized by a 2D honeycomb lattice with weak interlayer coupling, came into the focus of modern solid-state research: it is a prime candidate for the realization of Kitaev physics and fractionalized quasiparticles [24], composed of itinerant and localized Majorana fermions [25–27]. Arguments were put forth that these exotic fractionalized excitations could exist at temperatures above the onset of magnetic order. Indeed, recent Raman [12, 28, 29], neutron scattering [30–33], and time-domain THz experiments [14] provided possible experimental evidence of fractionalized excitations. However, an alternative scenario to explain the excitation continuum in terms of strong magnetic anharmonicity and a concomitant magnon breakdown was proposed by Winter *et al* [34]. Further strong support for the existence of fractionalised spins comes from the observation of a half-integer thermal quantum Hall effect [35].

In this manuscript, we present a detailed characterization of the exotic and strongly hysteretic structural phase transition in α -RuCl₃, where the stacking sequence of the vdW-coupled molecular layers is changed and the symmetry is lowered on increasing temperatures. After a characterization of the structural phase transition by thermal expansion experiments, we provide detailed combined terahertz (THz), far-infrared (FIR), and mid-infrared (MIR) reflectivity and transmission experiments from 1 meV to 1 eV in a wide temperature range. The main motivation of this work is to unravel the nature of the excitations by following the temperature dependence of the different modes across the structural phase transition to see if specific modes depend on symmetry or stacking sequence. This is specifically true for the THz excitations and for the orbital excitations in the MIR regime, where so far no consensus exists. We provide experiments on reflectivity and transmittance across the phase transition to study the temperature evolution of specific phonon modes and orbital excitations. From this, we try to assign the level splitting of the $4d$ electrons in the local electric field. Our findings cannot be explained based on existing theoretical models. We report on a complex THz spectrum, which possibly is of mixed electric and magnetic dipolar character and may indicate an underlying Kitaev physics. Significant differences to low-lying continua as observed in Raman and neutron scattering are discussed. In addition, we document the appearance of a new electronic

excitation in a narrow temperature range just across the structural phase transition. We propose that this finding indicates changes in the electronic density of state when shifting neighbouring layers of the vdW heterostructure, as has recently been reported for graphene [17, 18]. Furthermore, we contribute to the ongoing controversy about the low-energy orbital excitations in α -RuCl₃ and make a proposal for the spin-orbital coupled level scheme.

2. Methods

High-quality α -RuCl₃ single crystals, used in this work, were grown by vacuum sublimation. Samples were synthesized by the two groups in Seoul and in Augsburg separately. Samples grown in Seoul are characterized in detail in [11, 32]. The magnetic (figure S1) and thermodynamic characterization (figure S2) of the Augsburg-grown samples is described in the supplementary material (stacks.iop.org/JPhysCM/30/475604/mmedia) [23]. All batches of as-grown samples—independent of size and thickness—behave very similar, concerning details of the structural phase transition as well as concerning the onset of magnetic order close to 7 K. The thermal-expansion experiments were conducted with a Quantum Design PPMS equipped with a compact and miniaturized high-resolution capacitance dilatometer. For these experiments we used a small platelet with a thickness of 0.024 mm oriented along the crystallographic c direction. Despite an increased experimental uncertainty, rather thin platelets were measured to gain direct evidence of the temperature evolution of changes in the stacking sequence, in order to avoid the influence of macroscopic domains of thick bulk crystals.

The samples for the optical experiments had a typical ab surface of $5 \times 3 \text{ mm}^2$ and thicknesses of approximately $25 \mu\text{m}$ up to 1 mm. Thicker samples had to be used to measure transmission in the THz and reflectivity in the FIR regime. Thinner samples of various thickness were used in transmission experiments at FIR and MIR frequencies. Time-domain THz transmission experiments were performed with the wave vector of the incident light perpendicular to the crystallographic ab plane using a TPS Spectra 3000 spectrometer. We measured time-domain signals for reference (empty aperture) and samples, from which power spectra were evaluated via Fourier transformation. FIR and MIR reflectivity as well as transmission experiments for energies from 10 meV to 1 eV were performed using the Bruker FT-spectrometers IFS113v and IFS66v/S, with appropriate sets of sources, beam splitters and detectors. CryoVac He-flow cryostats allowed varying the sample temperature from 5 to 295 K. All IR experiments were performed with the incident wave vector perpendicular to the molecular stacks, i.e. parallel to the crystallographic c direction. For all reflectivity experiments, we used gold mirrors as reference. To convert the reflectivity spectra into the complex dielectric permittivity $\varepsilon(\omega) = \varepsilon'(\omega) - i\varepsilon''(\omega)$ we utilized the Kramers–Kronig constrained variational method, which was developed by Kuzmenko [36] and is included in the RefFIT program [37]. The use of this approach allows to obtain real and imaginary part of the complex permittivity $\varepsilon(\omega)$ without

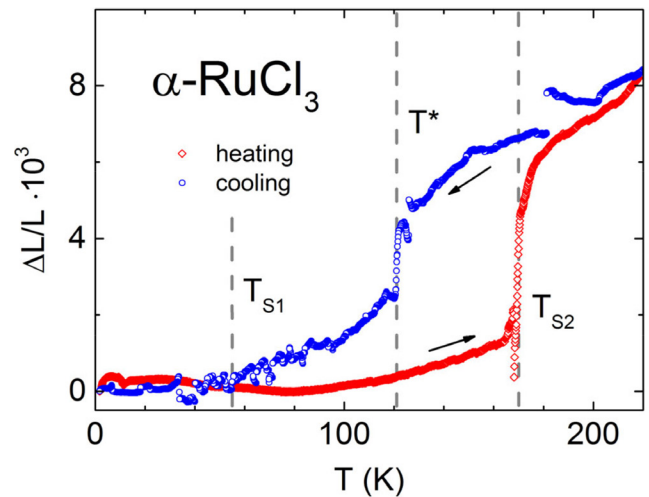


Figure 1. Temperature dependence of relative length changes $\Delta L/L$ in α -RuCl₃. The thermal expansion was measured perpendicular to the molecular stacks, i.e. along the crystallographic c direction, on heating (rhombs) as well as on cooling (circles). The length changes were scaled at 1.8 K. Vertical dashed lines indicate the three characteristic temperatures of the two-step hysteresis behaviour, following the notation of [11]. The large experimental uncertainties result from the fact that we used a sample with a thickness of $24 \mu\text{m}$ only. The kinks at T_{S2} and T^* are not reproducible and probably result from thermal fluctuations close to the first order phase transition. These experiments have been performed on samples grown in Augsburg.

the need of specific extrapolations at the low- and high-frequency edges of the measured reflectivity spectra. For the analysis of eigenfrequencies, damping and oscillator strengths of phonons and orbital excitations, observed in transmission as well as in reflectivity experiments, we used the RefFIT program [37]. Lorentzian profiles of the modes provided the best fits.

3. Experimental results

3.1. Thermal expansion

To gain insight into the nature of the structural phase transition of α -RuCl₃ and to understand its hysteretic behaviour, we performed thermal-expansion experiments, measuring length changes along the crystallographic c direction on thin samples. These experiments were stimulated by x-ray results of Park *et al* [11] reporting on a two-step ordering process of this layered structure. As we want to correlate observations of shifts of eigenfrequencies or temperature-dependent damping effects of excitations with the structural phase transition, these thermal expansion experiments are of prime importance.

Figure 1 documents a heating and cooling cycle of thermal expansion experiments along the c direction from low-temperatures up to 220 K. The temperature dependent length changes were scaled to 1.8 K, the lowest temperature of these experiments. Indeed, the detected length changes reveal a characteristic two-step ordering process. On cooling, the thermal expansion perpendicular to the molecular stacks exhibits conventional anharmonic behaviour down to a temperature of

121 K. At this temperature, the sample abruptly shrinks along the c direction and then continuously contracts down to 55 K. On heating, the sample remains in its low-temperature phase until the c axis abruptly expands at 170 K. This thermal expansion happens in a narrow temperature range and this abrupt structural change is monitored in the heat capacity experiments (see figure S2 of the supplementary material [23]).

The characteristic temperatures determined in this experiment, namely $T_{S1} = 55$ K, $T_{S2} = 170$ K and $T^* = 121$ K are close to those reported in [11] for the Seoul samples. In the temperature regime investigated, the overall thermal expansion is of the order of 1%, in perfect agreement with the length changes of the crystallographic c axis, which also amounts approximately 1% in the respective temperature regime [11]. We would like to recall that the main hysteresis of the structural phase transition in α -RuCl₃ is located between T^* and T_{S2} . However, on cooling only 50% of the length changes along c happen abruptly at T^* , while the remaining 50% continuously evolve on further cooling down to T_{S1} .

It is a characteristic feature of this phase transition that it resembles a two-step process on cooling when adapting the low-temperature rhombohedral phase, while it reveals a one-step process on heating, restoring the high-temperature monoclinic phase. It seems natural to assume that the temperature-induced changes of the crystallographic c direction mainly depend on the stacking sequence. On cooling, these changes happen partly at T^* and then the stacking continuously adapts a hexagonal AB sequence at T_{S1} , while on heating ABC type stacking is abruptly restored at T_{S2} . Recently, similar thermal expansion experiments as function of hydrostatic pressure have been performed by He *et al* [15], focusing on sample dependencies. These results also show an extended hysteresis of the structural phase transition between 66 and 168 K, with a similar size of the over-all effect of the thermal expansion along the c axis. However, the authors of [15] did not observe the two-step hysteresis documented in figure 1.

3.2. The dielectric response of α -RuCl₃ from the THz to the MIR regime

In this work, we provide a detailed investigation of the phonon properties and of spin-orbital excitations in a broad frequency range as function of temperature: We monitor the eigenfrequencies when passing the structural phase transition, to detect significant shifts of the modes, possible splittings or the appearance of new modes indicating symmetry-lowering transitions. This procedure allows detecting if a specific mode depends on the overall crystal symmetry and on the stacking sequence or rather on the symmetry of a single molecular stack. These measurements are motivated by three distinct open questions, highly relevant to the physics of α -RuCl₃: (i) Do optical remnants of the Kitaev-like spin-liquid state show up in THz experiments. If so, do the fractionalized excitations depend on the over-all structure of the compound? (ii) So far, there is no agreement between theory and experiment on the level splitting of the ruthenium $4d$ orbitals. Again, it seems important to check if the orbital excitations depend on the structure and are different in the low and high-temperature

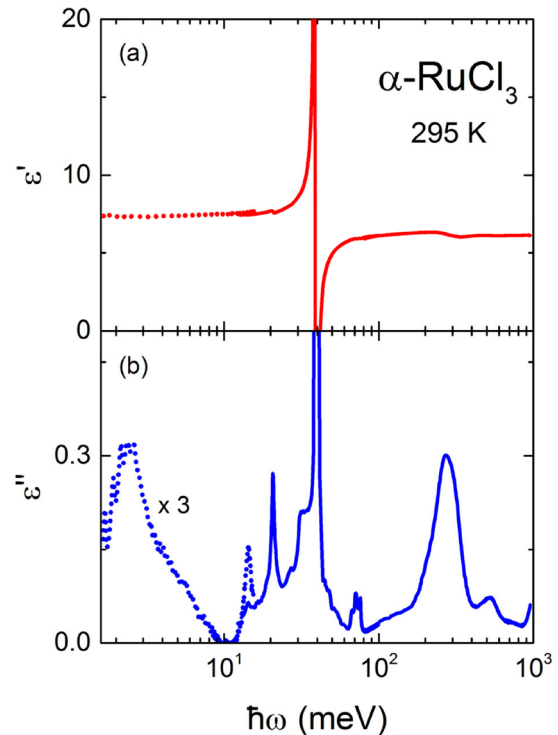


Figure 2. Low-energy dielectric response of α -RuCl₃. Energy dependence of (a) dielectric constant ϵ' and (b) dielectric loss ϵ'' at room temperature from 1 meV to 1 eV in semi-logarithmic representation. All spectra were measured with the incident light perpendicular to the molecular stacks. The spectra plotted with dashed lines were derived from time-domain THz spectroscopy in transmission and have been multiplied by a factor of three for better visibility. The solid lines result from Kramers–Kronig consistent reflectivity and transmission experiments in the FIR and MIR range. The strongest spin-orbital excitation close to 300 meV, is visible only in the real part as tiny anomaly. In [13, 38] this anomaly in the complex dielectric constant has been assigned as charge gap. The transmission experiments in the THz range were performed on Seoul-grown crystal, the transmission in the FIR and MIR spectral range was measured with Augsburg-grown samples of various thickness.

phase. (iii) We also wanted to contribute to the question about the optical band gap. The majority of publications point towards a gap of order 1 eV, while transport experiments favour charge gaps of the order 0.1 eV.

To provide an overview over phonon and electronic excitations in α -RuCl₃, figure 2 shows the energy dependence of the real (figure 2(a)) and imaginary part (figure 2(b)) of the dielectric constant from 1 meV up to 1 eV. This broadband result represents the outcome of combined THz, FIR and MIR measurements, analysing both, transmission and reflectivity using a series of crystals of different thickness ranging from ~ 25 μ m to ~ 1 mm. The real part of the dielectric response below 1 eV shows only one phonon-like excitation close to 40 meV. Only this phonon mode carries considerable dielectric strength $\Delta\epsilon \sim 1$, while all the other modes have small dipolar weight. In the imaginary part of the dielectric response, a number of excitations from 1 meV up to 1 eV are visible. Reschke *et al* [13] published a similar spectrum of the dielectric response previously. The absorption coefficient at FIR and MIR frequencies has also been published by

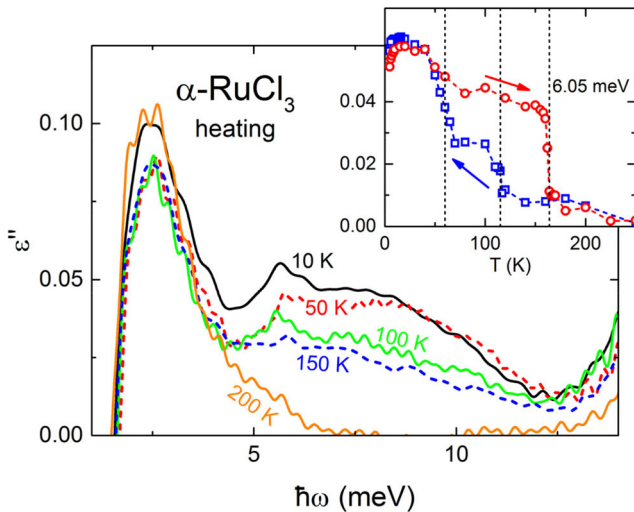


Figure 3. Energy dependence of the dielectric loss in α - RuCl_3 in the THz regime. These data have been taken in transmission on heating for a series of temperatures between 10 and 200 K on Seoul-grown samples. The inset displays the temperature dependence of the dielectric loss at 6.05 meV for a heating and cooling cycle and visualizes the two-step nature of the structural phase transition on cooling. In this energy regime, the THz loss is high in the rhombohedral low-temperature phase and approaches zero in the monoclinic high-temperature phase.

Hasegawa *et al* [38], including first-principle calculations of the phonon properties of α - RuCl_3 . Biesner *et al* conducted a detailed study of the pressure dependence of the conductivity spectrum up to 1.5 eV [39].

The study of temperature dependencies of excitations as documented in figure 2(b) will be the main outcome of this work. So far, these excitations cannot be uniquely assigned. It is the main motivation of this work to unravel their origin and nature by following these excitations across the structural phase transition. In what follows we discuss the temperature evolution of the spectra in the different frequency regimes, i.e. at THz, FIR and MIR frequencies. Remnants of Kitaev physics are expected below 10 meV, phonon modes will dominate between 10 and 50 meV, while beyond this energy, on-site spin-orbital excitations between different electronic levels of the ruthenium $4d^5$ electrons are expected. One also should have in mind that the question concerning the size of the electronic band gap is not finally solved.

3.2.1. Excitations in the THz regime: remnants of Kitaev physics? We specifically discuss the THz excitations in the paramagnetic regime to identify possible signatures of fractionalized excitations of the Kitaev-type spin-liquid. Figure 3 shows the frequency dependence of the dielectric loss of α - RuCl_3 for temperatures between 10 and 200 K when passing the structural phase transition. The well-defined mode close to 2.5 meV with width ~ 2 meV is temperature independent and exists in the high and low-temperature phase. The steep and well-defined onset of dielectric loss at low energies is compatible with the existence of a gap of ~ 1 meV in the excitation spectrum. A second excitation band, which extends from 4 meV up to 12 meV, only occurs in the low temperature

rhombohedral phase. Both excitations carry low optical weight and are only observable in transmission experiments on thick (~ 1 mm) samples. The increase of the loss towards high frequencies beyond 10 meV stems from the phonon mode, which is located close to 15 meV (figure 2(b)) and has also been observed by neutron scattering (see supplemental information of [23]).

As documented in figure 3, significant temperature-induced spectral changes appear at excitation energies from 5 to 12 meV, where a broad hump evolves on decreasing temperatures. Following the temperature evolution of the dielectric loss close to 6 meV, we find the characteristic hysteresis due to the phase transition, which is documented by the thermal expansion experiments (figure 1): Only minor changes appear below 60 K, while above 170 K this excitation is zero within experimental uncertainty (see inset of figure 3). Over-all this intensity is comparable to observations of high-energy intensity from itinerant Majorana fermions in the range from 6 to 12 meV in neutron scattering experiments [32]. These intensities decrease on decreasing temperature and vanish for $T > 125$ K. However, in neutron scattering these intensities have not been correlated with the structural phase transition. It also has to be mentioned that phonon intensity close to 7 meV was identified in these neutron-scattering experiments (see supplemental information of [23]). Contrary to the results presented in figure 3, this phonon intensity is increasing with increasing temperature and strongest at 200 K.

3.2.2. Excitations in the FIR regime: phonons. From published experimental work so far, it is evident that the phonon modes are determined mainly from the D_{3d} symmetry of an isolated molecular stack. In the 2D honeycomb-type trihalides, phonon modes so far were detected between 10 and 50 meV: Early IR experiments on α - RuCl_3 were published by Fletcher *et al* [3] and Guizetti *et al* [40]. Later on, combined reflectivity and transmission results were reported by Little *et al* [41] and finally, a detailed analysis of phonon excitations was presented by Reschke *et al* [13] and by Hasegawa *et al* [38]. IR spectroscopy results on a variety of isostructural tri-halides have been published by Emeis *et al* [42], Bermudez [43], and Borghesi *et al* [44]. In all these experiments, no one-phonon excitations are reported below 10 and beyond 50 meV. This is in accord with first-principle calculations of phonons of α - RuCl_3 by Hasegawa *et al* [38] and of non-magnetic RhCl_3 from Wolter *et al* [45].

We would like to recall that assuming D_{3d} symmetry in IR spectroscopy two A_{2u} and three E_u modes are expected [38, 43]. In clear distinction, in rhombohedral $R\bar{3}$ symmetry three A_u and three E_u modes, while in the high-temperature monoclinic $C2/m$ phase four A_u and five B_u modes should be observed [46]. To search for these modes and for the possible appearance of new modes at the structural phase transition, we performed new detailed and systematic transmission experiments.

In this work, we will focus on the absorption as measured in the FIR regime. Reflectivity experiments were performed previously [13] and essential results are shown in figure S3 of the supplementary material [23]. Figure 4 shows the transmission

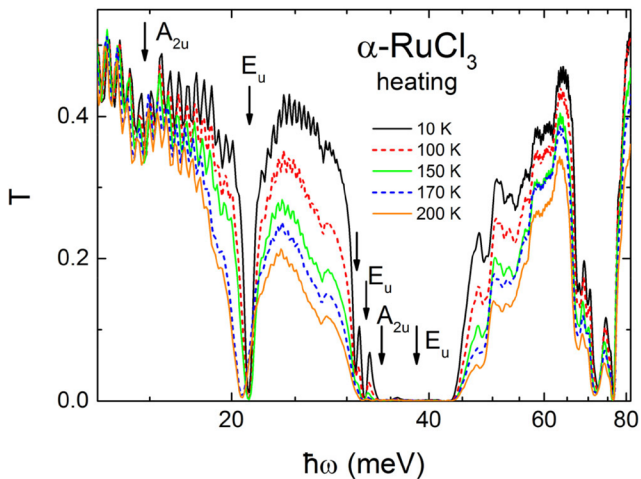


Figure 4. Energy dependence of the transmission T in α - RuCl_3 for photon energies from 10 to 80 meV. Transmission spectra on a semi-logarithmic plot for temperatures between 10 and 200 K on heating across the structural phase transition. The arrows indicate one-phonon excitations in A_{2u} and E_u symmetry in accordance with theoretical predictions from [38]. In the geometry chosen for these experiments, with the incident wave perpendicular to the ab plane, we expect only three E_u modes assuming D_{3d} symmetry of a single molecular stack. A_{2u} modes can only become visible if the sample is slightly misaligned or from misaligned domains. The strong absorption band above 70 meV is a matter of dispute. The mode at 31 meV remains unassigned. For these experiments, Seoul-grown samples were used.

as measured on heating for energies from 10 to 80 meV and for temperatures from 10 to 200 K. In the FIR regime, we detect a series of rather strong absorption bands. Figure 4 also provides experimental evidence that—with the exception of small shifts and concomitant changes of the damping of the 21 meV phonon—no specific symmetry changes of phonon modes, when crossing the structural phase transition, appear. Hence, it seems justified to assume that D_{3d} symmetry of a single molecular stack governs the lattice dynamics of α - RuCl_3 . In this case and in the geometry chosen in the experiment documented in figure 4, we expect three E_u modes. A_{2u} modes can only be detected by a misalignment of the sample or by misaligned domains within the sample. Theoretically, IR active modes of E_u symmetry are expected at 20.7, 33.7 and 38.3 meV, while A_{2u} modes have been predicted at energies of 15.1 and 35.2 meV [38].

The arrows in figure 4 indicate the experimentally observed absorption bands located at 14.7 and 34.2 meV for the A_{2u} modes and at 21.3, 32.0 and 39.2 meV for the E_u modes. All these eigenfrequencies are close to the theoretical predictions [38]. We also detect one extra mode close to 31 meV, which cannot be assigned and possibly corresponds to the lower symmetry of the real 2D crystal lattice. The real crystal symmetry is lower than that of the assumed D_{3d} symmetry and in total six modes are expected in the rhombohedral and 9 modes in the monoclinic phase. Possibly the majority of these modes is missed due to low dipolar weight. All the other small anomalies and spikes are due to two-phonon process or—at low energies—due to interference pattern of scattered light between the sample surfaces.

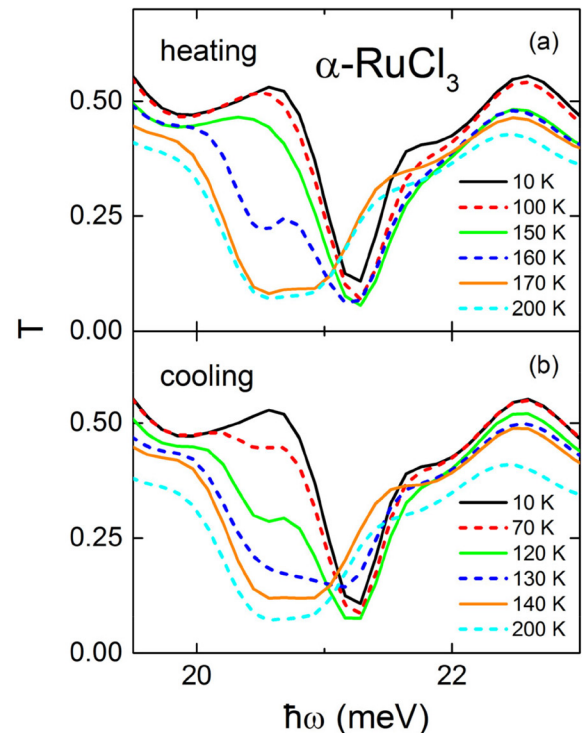


Figure 5. Transmission spectra in α - RuCl_3 close to the phonon mode at 21 meV for a series of temperatures. The energy dependent transmission is reported on crossing the structural transition during heating (a) and cooling (b). Note the extended two-phase region on cooling, which extends at least from 70 to 130 K.

A remark has to be made concerning the strong absorption feature at 73 meV (see figure 4). If one-phonon processes in the tri-halides are confined to energies below 50 meV, this significant absorption in α - RuCl_3 has to be ascribed to multi-phonon processes or to an orbital excitation. The former explanation has been proposed in [38]. We think that multi-phonon processes cannot explain the dominant absorption band at 73 meV. Two-phonon excitations, which extend to higher energies, are rather weak [43, 44]. For example, two-phonon modes reported for isostructural CrCl_3 , indeed have been observed in transmission experiments [43], but appear as very weak absorption bands only. Hence, one should take into consideration that this strong absorption band at 73 meV stems from an electronic transition and only the overlaying fine structure results from multi-phonon process. On the other hand, taking existing theoretical information so far, no orbital or spin-orbital excitations should exist below 100 meV. In the most detailed quantum chemistry calculations [47] the excitations between the spin-orbital split ground state appear at much higher energies.

Figure 5 documents the sensitivity of the specific phonon mode at 21 meV on structural changes of α - RuCl_3 when passing from the low-temperature rhombohedral to the high-temperature monoclinic phase. At first sight (see the transmission documented in figure 4), the phonon modes undergo no significant changes from room temperature down to the lowest temperatures. Specifically, no new modes become visible beyond experimental uncertainty [13], although the very weak dipolar weight of some of these vibrations and the

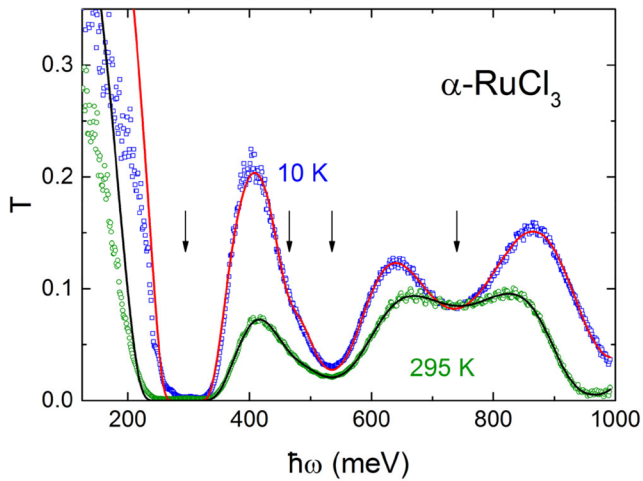


Figure 6. Transmission T in α - RuCl_3 for photon energies from 150 meV to 1 eV. As the eigenfrequencies of the transmission bands only weakly depend on temperature, transmission spectra are shown at 10 and 295 K only. The solid lines represent fits of the transmission profile using Lorentzian-type fits. The vertical arrows indicate excitation energies at 10 K for four bands that have been assumed in these fits (see text). The strong decrease of transmission close to 200 meV, was analysed in terms of a direct allowed transition across the optical band gap [13]. These experiments were conducted on Augsburg-grown samples.

strong multi-phonon scattering hamper the identification of new modes. Nevertheless, the phonon mode close to 21 meV reveals significant changes in eigenfrequency and damping clearly beyond experimental uncertainties and is sensitive to structural changes and to the stacking sequence.

Figure 5 shows some representative transmission scans for heating (figure 5(a)) and cooling (figure 5(b)). The narrow mode at 21.2 meV is characteristic for the low-temperature rhombohedral phase, while an excitation at 20.7 meV with significantly larger damping is the fingerprint of the high-temperature monoclinic phase. In a wide temperature regime, these two excitations coexist, documenting the first-order character of the structural phase transition, with a wide heterogeneous coexistence regime of both phases. On heating, the narrow mode exists up to at least 150 K and then rapidly transforms into the excitation characteristic for the monoclinic phase, which is fully developed at 170 K. On cooling, traces of the high-temperature mode still are visible down to 70 K, fully compatible with the hysteresis documented in the thermal-expansion experiments shown in figure 1. On cooling the two-phase region extends from 130 down to 70 K, while on heating the two-phase region is limited to a narrow temperature range around 160 K.

It seems important to note that an isosbestic point appears close to 21 meV indicative of a well-established two-phase regime. This phonon mode turns out to be an ideal probe for the crystallographic symmetry and the stacking sequence of the samples under consideration. A narrow line signals the rhombohedral phase with AB stacking. A broad line at slightly lower frequencies is the fingerprint of the monoclinic high-temperature phase. A splitting of this mode is a characteristic

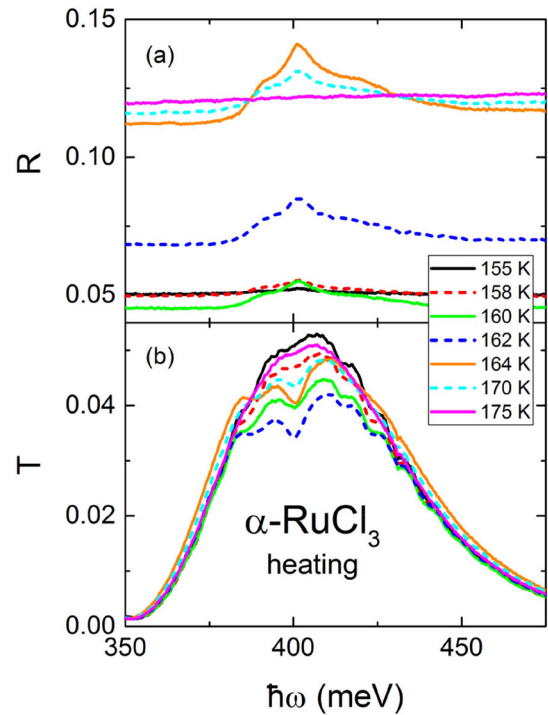


Figure 7. (a) Mid-infrared reflectivity R and (b) transmission T in α - RuCl_3 around 400 meV. Reflectivity and transmission are shown for a series of temperatures from 155 to 175 K on heating. Exactly at this temperature regime, the crystal transforms from the low-temperature rhombohedral to the high-temperature monoclinic structure. The transmission is identical in the high- and low-temperature ordered phases. However, the MIR reflectivity changes by a factor of 2.5 between high and low-temperature phases. The reflectivity experiments documented in (a) were performed on Seoul-grown samples, while the transmission experiments of (b) were conducted on Augsburg-grown samples.

feature of samples with stacking faults and mixed monoclinic and rhombohedral phases.

3.2.3. Excitations in the MIR regime: onsite orbital excitations. Finally, we discuss transmission and reflection experiments on α - RuCl_3 in the MIR regime. Electronic excitations dominate the frequency dependent complex dielectric constant beyond 100 meV. These excitations are very weak, as they are parity and spin forbidden. They gain dipolar intensity only via p - d coupling or via coupling to lattice vibrations. Hence, these excitations are almost invisible in reflectivity and have to be studied in transmission geometry. Figure 6 shows the transmission spectra between 100 meV and 1 eV as observed at 10 K and at 295 K. At first sight, at both temperatures one can observe three characteristic transmission bands. This interpretation is in accord with earlier reports [13, 38, 48]. However, a closer inspection indicates a fourth absorption band just above 400 meV, which is documented by a strong asymmetry of the transmission maximum between first and second absorption band. The transmission profiles significantly sharpen on decreasing temperatures indicating strongly decreasing damping. The transmission of the low-frequency band approaches zero, indicating that in this energy regime the sample was too

thick. Sandilands *et al* [49] have studied spin–orbit excitations in detail. In agreement with earlier results [40, 50], these modes were assigned to excitations from the t_{2g}^5 ground state to excited spin–orbit states of $t_{2g}^4 e_g^1$ character close to 0.3, 0.5 and 0.7 eV. Reschke *et al* [13] and Hasegawa *et al* [38] performed related studies. The latter authors also discussed the possibility that the lowest excitation close to 300 meV indicates the onset of the optical band gap.

The transmission spectra have been fitted with Lorentzian profiles using the RefFit routine [37]. In figure 6 the fits are indicated as solid lines. At room temperature, we observe four electronic absorption bands centred at eigenfrequencies of 277, 474, 542 and 752 meV and with characteristic dampings of 15, 115, 137 and 276 meV, respectively. At 10 K, these absorption bands are located at 294, 465, 536 and 740 meV with damping factors of 11, 60, 111 and 224 meV. On cooling, the lowest frequency band undergoes a significant blue shift, a hallmark of electronic transitions coupled to vibronic states. There are only minor temperature-induced shifts for the absorption bands close to 465 and 536 meV, while we found a conspicuous red shift for the high-frequency band.

On decreasing temperatures, the damping of the lowest two absorption bands decreases up to a factor of two, while the damping of the higher frequency bands decreases by approximately 20% only. It is interesting to note that the intensity of these absorption bands are temperature independent and remain constant within less than 10%. These temperature-induced shifts and broadening effects are continuous and do not seem to be significantly influenced by the structural phase transition or by changes in the stacking sequence. We conclude that the symmetry of the crystal electric field of a single molecular stack determines these on-site absorption bands.

Figure 6 also signals a strong increase of the transmission below 200 meV. In [13] this absorption edge has been interpreted as the band edge for electronic transitions across the optical band gap and seems consistent with band gaps as derived from temperature dependent dc resistivity results [50]. This optical gap also shows a strong blue shift on decreasing temperatures. However, this interpretation is at odds with a number of reports claiming gap values of the order 1 to 2 eV [48, 51].

Here we want to document the occurrence of a new electronic transition close to 400 meV, which appears only in a very narrow temperature range on heating, when the crystallographic structure changes from the low-temperature rhombohedral into the high-temperature monoclinic phase. This electronic excitation is clearly visible in reflectivity (figure 7(a)) as well as in transmission (figure 7(b)). It only exists (or is IR active) in the heating cycle in the narrow temperature range between 155 and 175 K, exactly in the transition region where the rhombohedral phase transforms into the monoclinic one (see figure 1). It is invisible in reflectance as well as in transmission for higher and lower temperatures in both fully ordered phases.

One plausible reason for its occurrence just in the phase-transition regime could be that this transition is fully spin and/or parity forbidden in the ordered phases and hence is invisible

in IR experiments, but becomes disorder-allowed just at the phase transition where the stacking sequence changes. In this structural phase transition, the stacking sequence changes most likely by a continuous shift of neighbouring molecular stacks. A highly intriguing explanation would be that the electron density of states changes when neighbouring stacks are shifted. A similar observation, namely that the electron density of a heterostructure strongly depends on the twisting angle of neighbouring layers has recently been reported for graphene [17, 18]. It is unclear, why we never were able to observe this extra excitation in cooling cycles. The extreme smearing out of this transition over more than 100 K could be a possible explanation. Of course, much more experimental and theoretical work is needed to document such a behaviour.

Figure 7 also provides experimental evidence for significant differences in changes of transmission and reflectance, when passing the structural phase transition. Figure 7(b) documents that the transmission is identical within experimental uncertainty in the high and low temperature phases. The excitation in reflectivity becomes apparent only when crossing the phase transition (figure 7(a)). However, this figure impressively documents the significant change in the overall reflectivity at MIR frequencies, which was documented earlier [13]. The reflectivity in the monoclinic phase with cubic ABC stacking is by a factor of 2.5 higher than the reflectivity in the rhombohedral phase with hexagonal AB stacking sequence. As outlined above, this dramatic change in reflectivity is a characteristic feature accompanying the change in the stacking sequence of α -RuCl₃ and can be observed from 1 meV up to 1 eV. It possibly indicates additional broadband reflectivity or absorption processes at the surface or at the interfaces of the vdW coupled molecular layers.

4. Discussion

In this work, we provide a detailed study of phononic, spin-orbital and orbital excitations in α -RuCl₃ by broadband optical experiments in the THz, FIR and MIR frequency range. We specifically focus on the temperature dependencies of eigenfrequencies and damping of these excitations when crossing the structural phase transition. Already at this point, it is clear that most of the modes are barely influenced by the structural phase transition and hence, mainly depend on the local environment of a single molecular stack. This is not true for the THz excitation at 7 meV, which becomes suppressed in the high-temperature monoclinic phase and for the phonon at 21 meV, which exhibit a significant shift of eigenfrequency when passing the structural phase transition.

4.1. THz excitations

In this frequency regime we expect signatures of fractionalized excitations of the Kitaev-type spin-liquid. The dielectric loss as documented in figure 3 reveals a temperature independent excitation close to 2.5 meV, which exits up to room temperature and a broad excitation around 7 meV, which only exists in the low-temperature rhombohedral phase. At first sight,

one could try to assign the low-frequency mode to an orbital transition between nearly degenerate orbitals. With the SOC constant of $\lambda \sim 100$ meV [30, 49] in mind, it seems unlikely to expect spin-orbital excitations below 10 meV, even assuming that the spin-orbital derived quartet and doublet states are further split into three Kramers doublets by a trigonal distortion of the octahedral CEF [52]. It seems interesting to note that low-frequency spin-orbital excitations have been observed in a number of spin-orbital coupled $3d$ transition-metal chalcogenides [53–56].

That the dielectric loss documented in figure 3 may indicate remnants of Kitaev physics, stems from a recent theoretical work from Bolens *et al* [57]. These authors calculated the low-frequency optical conductivity of Kitaev materials assuming an interplay of Hund’s coupling, spin-orbit coupling, and crystal-field effects. Using realistic parameters for α -RuCl₃ they predict a low-frequency peak of magnetic dipolar response close to 1 meV, a dominant peak of electric dipolar nature close to 6 meV and a low-frequency gap value close to 0.3 meV. This predicted spectrum bears striking similarities with the loss spectrum shown in figure 3 just above the onset of magnetic order at 10 K, with a gap-like feature close to 1 meV and two peaks located at 2.5 and 7 meV. However, a number of open questions remain: The low-frequency peak has almost no temperature dependence up to room temperature. The 7 meV peak only exists in the low-temperature phase and is absent in the high-temperature monoclinic phase. Finally, nothing is known about a possible magneto-electric coupling in this material. However, weak anisotropic magneto-electric effects at audio frequencies were reported recently [58].

It seems also important to compare the present experiments with published THz work. With the focus on the possible occurrence of a continuum due to fractionalized excitations, Wang *et al* [14] discussed this frequency regime in detail. To avoid possible interference with spectral changes driven by the structural phase transition, the focus of the analysis of the THz spectra in [14] was on temperatures below 60 K and only difference spectra were shown. These studies were extended to external magnetic fields up to 15 T. Detailed investigations of the THz regime between 1 and 6 meV have also been published by Little *et al* [41] and by Shi *et al* [59]. Very recently the field evolution of magnon excitations in α -RuCl₃ were studied by Wu *et al* [60], with the focus on difference spectra between 8 and 4 K. For frequencies between 1–6 meV and temperatures from 2 K to room temperature, Little *et al* [41] reported conductivity spectra similar to the findings shown in figure 3. THz conductivity spectra published by Shi *et al* [59] show a broad hump close to 4 meV, weakly depending on temperature and external magnetic field. The broad conductivity hump still exists at 7 T and persist up to room temperature.

We also try to compare our THz results with those deduced from Raman spectroscopy [12, 28] and from inelastic neutron scattering experiments [30, 32, 61]. Utilizing Raman scattering techniques, Sandilands *et al* [28] and Glamazda *et al* [12] report on a low-temperature continuum extending up to ~ 25 meV, certainly much wider in energy than the THz observations of this work documented in figure 3. Theoretically this

fermionic intensity exhibits significant temperature dependence, but still is expected to be observable at room temperature [29]. In neutron scattering, at low temperatures the absence of scattered intensity below 2 meV confirmed a gap in the magnetic excitation spectrum [30]. In addition, a broad peak was observed, centred at approximately 5 to 8 meV [30, 32, 61], which is not too far from the findings reported in figure 3. This peak has maximum intensity at low temperatures and continuously decreases on increasing temperature. It is worth mentioning that specifically the inelastic intensity between ~ 6 and ~ 12 meV, reported by Do *et al* [32], resembles a temperature dependence quite similar to that documented in figure 3 in a similar frequency range. This inelastic neutron scattering intensity vanishes for temperatures above 125 K and has been interpreted to result from high-frequency itinerant Majorana fermions. However, a correlation of this excitation with the structural phase transition has not been investigated. All Raman and neutron scattering studies cited above, provide no experimental evidence for a temperature-independent peak-like structure close to 2 meV in the paramagnetic phase, as evidenced in figure 3. The striking temperature independence of its optical strength discards an interpretation in terms of fractionalized excitations. A possible explanation of this excitation could be found in soft phonon modes of weakly coupled vdW layers. However, no information concerning such modes to date is available in these layered compounds.

4.2. Phonons

So far our phonon results are in reasonable agreement with published work [13, 38] and the over-all phonon properties of α -RuCl₃ can well be described by D_{3d} symmetry of a single molecular stack. We detected one mode close to 31 meV, which cannot be assigned and possibly indicates lower symmetry of the 3D crystal. We identify one phonon mode at 21 meV (figures 4 and 5), which significantly changes eigenfrequency and damping when crossing the structural phase transition and hence, indicates a dependence on symmetry and the stacking sequence. Furthermore, we find a strong absorption band at 73 meV, which so far was interpreted in terms a multiphonon absorption [38]. We however, tend to interpret this mode as orbital excitation.

As mentioned earlier, in octahedral symmetry and strong crystal field, the ground state will be a t_{2g} triplet state with spin $S = 1/2$, which under SOC further splits into a low-lying doublet ($J = 1/2$) and an excited quartet ($J = 3/2$). Deviations from cubic crystal-field symmetry will further split these states into three Kramers doublets and we speculate that the absorption band close to 73 meV corresponds to a transition from the ground state to the lowest excited doublet. In literature there exist only very few reports of excitations of ruthenium ions with d^5 configuration in octahedral fields. Geschwind and Remeika [52] measured Ru³⁺ in α -Al₂O₃, which substitutes Al and is located in an octahedral crystal field with trigonal distortion. In these experiments, the level splitting due to deviations from cubic symmetry was of order 100 meV, not too far from the excitation frequency observed in our experiments.

Estimates of the level splitting due to the trigonal distortion in α -RuCl₃ range from 12 meV from an analysis of x-ray absorption spectroscopy [62], to 50 meV from energy band-structure calculations [63] and 70 meV from quantum chemistry calculations [47], even up to ~ 100 meV, the order of spin-orbit coupling, from an analysis of the anisotropy of the g -values [10]. Further experiments and model calculations will be necessary to settle this dispute and to help identifying the nature of this 73 meV excitation in α -RuCl₃.

4.3. Orbital excitations

So far, in optical spectroscopy three orbital excitations were identified located close to 300, 500 and 700 meV [13, 38, 49]. They were assigned to excitations of the Ru d^5 electrons from the t_{2g}^5 ground state to excited spin-orbit states of $t_{2g}^4 e_g^1$ character. The excitation between the spin-orbit split ground state has only been detected by Raman spectroscopy close to 145 meV [49] and was not identified by any reported IR experiment. A spin-orbit splitting of the order 195 meV was deduced from inelastic neutron-scattering experiments [30]. Neither Raman nor neutron experiment were able to detect any further splitting of this doublet to quartet transition, due to the trigonal distortion of the crystal field. As outlined above, experimental evidences of this trigonal splitting range from 12 to 100 meV.

Based on the present experiments and on our analysis as detailed above, we identify five orbital excitations below 1 eV: At room temperature these are located at 73, 277, 474, 542 and 752 meV. However, we would like to state that this interpretation is not consistent with *ab initio* calculations, where these $t_{2g}^5 \rightarrow t_{2g}^4 e_g^1$ excitations have been predicted for energies well beyond 1 eV. Yadav *et al* [47] reported detailed electronic structure calculations and corresponding energies of electronic excitations. These calculations do not support the interpretation of the excitations between 100 meV and 1 eV as being due to $t_{2g} \rightarrow e_g$ transitions, which are computed at energies significantly beyond 1 eV. According to these quantum chemistry calculations, only two excitations should be observed at low energies. Depending on details of the model and the assumed symmetry, the spin-orbit splitting is of order 200 meV, with a trigonal splitting of 70 meV [47].

In figure 8 we propose a scenario assuming a trigonal distortion of the octahedral crystal field, which split the excited quartet into two doublets, resulting in three Kramers doublets as shown in figure 8(c). So far, from Raman [49] and neutron scattering experiments [30] it has been assumed that the spin-orbit splitting Δ amounts 150–200 meV. No indication of a second transition was reported. Values of the trigonal splitting, here $\Delta_2 - \Delta_1$, range between 10 and 100 meV [10, 47, 62, 63]. The fact that only one transition is observable was interpreted as being due to an almost cubic symmetry with a very small trigonal distortion [62]. In the related Kitaev-type Iridates with stronger spin-orbit coupling, onsite $d-d$ excitations have been observed well below 1 eV and the trigonal splitting was estimated as being ~ 100 meV [64].

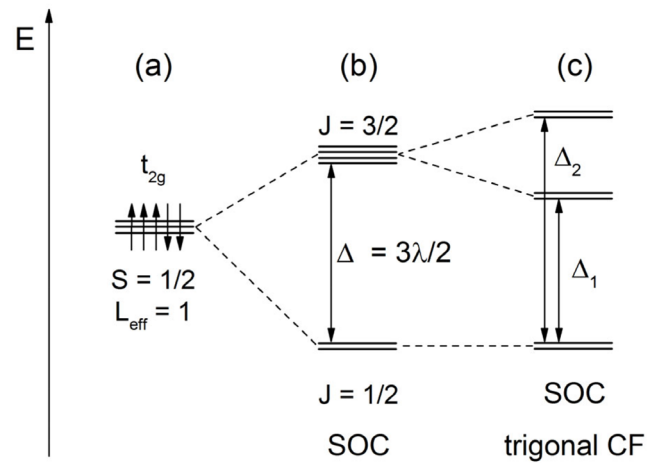


Figure 8. Spin-orbital excitation spectrum of α -RuCl₃ in an octahedral crystal field. (a): Low spin t_{2g} ground state, forming a state with an effective angular momentum of $L_{\text{eff}} = 1$ and spin $S = 1/2$. (b) Spin-orbit coupling splits this ground state into a lower doublet and an excited quartet. (c) Further trigonal distortion yields three Kramers doublets. In recent literature estimates of Δ are of order 200 meV, while values of the trigonal splitting $\Delta_2 - \Delta_1$, range from ~ 10 to 100 meV (see text).

With the level scheme indicated in figure 8 and with the excitation energies detected in this work, one interpretation is that $\Delta_1 \sim 70$ meV and $\Delta_2 \sim 250$ meV correspond to excitations between the three Kramers doublets. Clearly these values are not compatible with results reported so far and would indicate a large trigonal splitting, not in accord with recent x-ray absorption spectroscopy results [62]. Alternatively, one could assume that the trigonal splitting is hidden within the first absorption band just below 300 meV and cannot be resolved. In this case the strong 70 meV absorption has to be interpreted as two-phonon absorption. The origin of the remaining three excitation energies remains unclear. So far, the remaining excitations have to be interpreted in terms of $t_{2g}^5 \rightarrow t_{2g}^4 e_g^1$ excitations, which however, is not supported by theory: from quantum chemistry electronic structure calculations, these excitations are expected well beyond 1 eV, which is true in $C2/m$ as well as in $P3_112$ symmetry [47]. In the latter symmetry, Yadav *et al* [47] even calculated the $t_{2g}^5 \rightarrow t_{2g}^3 e_g^2$ transition at 920 meV, well below excitations from the ground state to the $t_{2g}^4 e_g^1$ levels. One has to keep in mind that the level scheme as outlined in figure 8 corresponds to a purely local picture of on-site excitations. This description strictly holds only in the case of Ru³⁺ diluted in an isolating host. α -RuCl₃ is a strongly correlated material and it is unclear how the band picture would change these atomic-like excitations.

4.4. Optical band gap

α -RuCl₃ is a good insulator and the majority of experimental and theoretical results point towards an optical gap of order 1 eV [48], but energy gaps of 1.9 eV determined from photoemission studies are also reported [51]. However, there are some arguments in favour of a much smaller charge gap of

order 100–300 meV [13, 38]. Figure 2 documents the frequency dependence of dielectric constant and dielectric loss of a good insulator, with no apparent free charge carriers even at room temperature. Any significant contribution of dc conductivity would result in a continuous increase of the dielectric loss towards low energies, which cannot be detected, even not down to 1 meV and even not at the highest temperatures investigated (figure 2(b)). The question, if the strong absorption edge close to 250 meV as indicated in figure 2(b) corresponds to the charge gap is far from being settled [13, 38]. It is worth mentioning that scanning tunnelling microscopy data showed an electronic energy gap of ~ 250 meV [21]. It has to be proven if the *in situ* cleaved α -RuCl₃ surfaces resemble the properties of the bulk crystal.

5. Conclusions

This manuscript reports on a detailed optical study of the temperature dependence of excitations in α -RuCl₃ in the THz, FIR and MIR frequency regimes. The optical investigations are complemented by measurements of the thermal expansion. It seems now well established that the structural phase transition in α -RuCl₃ signals changes in the stacking sequence of the molecular layers, but that the structure of the molecular Cl–Ru–Cl layers remain essentially identical. By comparing with related tri-halide compounds, it seems plausible to assume that an AB stacking in the rhombohedral phase at low temperatures is followed by an ABC stacking sequence in the monoclinic high-temperature structure. The phase transition is of strongly first order and exhibits a hysteresis extending between $T_{S1} = 55$ K and $T_{S2} = 170$ K. In addition, the cooling cycle of the hysteresis exhibits a clear two-step behaviour.

In the optical experiments we document that this prominent two-step relaxation of the *c* axis is mirrored in the reflectance and transmittance at all frequencies investigated, namely at THz, FIR and MIR frequencies. In clear distinction, the eigenfrequencies of phonon modes as well as of spin-orbital excitations reveal no significant influence of the structural phase transition, with the exception of a broad excitation evolving in the THz regime in the rhombohedral phase and a clear shift of the phonon mode at 21 meV.

Focusing on the phononic and electronic excitations below 1 eV reported in this work, a number of ambiguities remain. In the THz regime at low temperatures, we found clear experimental evidence for two excitations close to 2.5 and 7 meV, including a gap-like cut-off frequency of 1 meV (figure 3). These results bear some similarities with recent calculations of polarization and spin correlation functions on the Kitaev honeycomb lattice [57] and, hence, could signal some remnants of Kitaev physics. There have been published Raman [28, 29], neutron scattering [30, 32, 61] and THz results [14, 41, 59, 60] focusing on the low-energy excitation spectrum in α -RuCl₃. Some of these studies report on a low-energy continuum. However, neither from the energy range nor from the temperature dependence, these reported results bear significant common universalities, which unambiguously point towards a fractionalized excitation spectrum of Majorana fermions. Of

course, one possible explanation could be that details of the microscopic interactions are strongly sample dependent and e.g. depend on the stacking sequence of the molecular stacks and hence, on the phase transition. Much more theoretical and experimental work is needed to unravel the low-energy excitation spectrum in this fascinating compound.

The phonon properties of α -RuCl₃ presented in this work can well be described by assuming D_{3d} symmetry of a single molecular stack and are in reasonable agreement with published results [13, 38, 39]. The phonon mode close to 21 meV is the only mode sensitive to the stacking sequence. A mode close to 31 meV remains unassigned. Finally, we observe a strong absorption band at 73 meV, which according to [38] is a multi-phonon absorption. We argue that for a two-phonon scattering process, the experimentally observed absorption is too strong and we favour an interpretation in terms an electronic transition.

The interpretation of the electronic transitions in α -RuCl₃ below 1 eV is far from being solved. We identified five spin-orbital excitations, which cannot be explained by published theoretical models. Much more theoretical and experimental work is needed to get estimates of the trigonal splitting and to assign the orbital excitations. This will be of fundamental importance to finally determine the strength of the spin-orbit coupling in α -RuCl₃.

In addition, we detected an electronic transition close to 400 meV. This excitation only appears on heating in a narrow temperature range, exactly at the transition from the rhombohedral into the monoclinic structure. This excitation could correspond to a spin and parity forbidden transition, which becomes disorder-allowed just in the temperature range of the structural transformation. A more appealing interpretation would be the hypothesis that these extra excitations correspond to drastic changes in the electronic density of states when during the structural phase transition neighbouring molecular stacks are shifted, similar to recent observations in graphene when twisting neighbouring layers [17, 18].

We conclude and have to admit that these detailed optical experiments on α -RuCl₃ created more open questions than have been solved. From our point of view, the striking excitations in the THz regime, which could be remnants of Kitaev physics and the unclear orbital-derived sub-gap excitation spectrum < 1 eV, deserve further theoretical here in α -RuCl₃, is a characteristic feature of a large number of layered tri-halides. It certainly would be interesting to study in detail this exotic phase transition in isostructural compounds.



Acknowledgments

We thank Philipp Gegenwart, Roser Valenti, Stephen Winter, and Igor Mazin for stimulating discussions and helpful comments. This research was partly funded by the Deutsche Forschungsgemeinschaft DFG via the Transregional Collaborative Research Center TRR 80 ‘From Electronic correlations to functionality’ (Augsburg, Munich, Stuttgart).

KYC was supported by Korea Research Foundation (KRF) Grants (No.: 2017012642). The work of MVE was funded

by a grant, allocated to the Kazan Federal University for the state assignment in the sphere of scientific activities (Contract number: #3.6722.2017/8.9).

ORCID iDs

Kwang-Yong Choi  <https://orcid.org/0000-0001-8213-5395>
Alois Loidl  <https://orcid.org/0000-0002-5579-0746>

References

- [1] Stroganov E V and Ovchinnikov K V 1957 *Vestnik. Leningr. Univ. Fiz. Khim.* **12** 152
- [2] Fletcher J M, Gardner W E, Hooper E W, Hyde K R, Moore F H and Woodhead J L 1963 *Nature* **199** 1089
- [3] Fletcher J M, Gardner W E, Fox A C and Topping G 1967 *J. Chem. Soc. A* **1038**
- [4] Brodersen K, Moers F and Schnering H G 1965 *Naturwissenschaften* **52** 205
- [5] Brodersen K, Thiele G, Ohnsorge H, Recke I and Moers F 1968 *J. Less Common Met.* **15** 347
- [6] Cantow H-J, Hillebrecht H, Magonov S N, Rotter H W, Drechsler M and Thiele G 1990 *Angew. Chem., Int. Ed.* **29** 537
- [7] Morosin B and Narath A 1964 *J. Chem. Phys.* **40** 1958
- [8] McGuire M A, Dixit H, Cooper V R and Sales B C 2015 *Chem. Mater.* **27** 612
- [9] McGuire M A, Clark G, Santosh K C, Chance W M, Jellison G E Jr, Cooper V R, Xu X and Sales B C 2017 (arXiv:1706.01796)
- [10] Kubota Y, Tanaka H, Ono T, Narumi Y and Kindo K 2015 *Phys. Rev. B* **91** 094422
- [11] Park S-Y et al 2016 (arXiv:1609.05690)
- [12] Glamazda A, Lemmens P, Do S-H, Kwon Y S and Choi K-Y 2017 *Phys. Rev. B* **95** 174429
- [13] Reschke S, Mayr F, Wang Z, Do S-H, Choi K-Y and Loidl A 2017 *Phys. Rev. B* **96** 165120
- [14] Wang Z, Reschke S, Hüvonen D, Do S-H, Choi K-Y, Gensch M, Nagel U, Rößm T and Loidl A 2017 *Phys. Rev. Lett.* **119** 227202
- [15] He M, Wang X, Wang L, Hardy F, Wolf T, Adelman P, Brückel T, Su Y and Meingast C 2017 (arXiv:1712.08511)
- [16] Wasse J C and Salmon P S 1999 *J. Phys.: Condens. Matter* **11** 2171
- [17] Cao Y et al 2018 *Nature* **556** 80
- [18] Cao Y, Fatemi V, Fang S, Watanabe K, Taniguchi T, Kaxiras E and Jarillo-Herrero P 2018 *Nature* **556** 43
- [19] Yang H, Kim S W, Chhowalla M and Lee Y H 2017 *Nat. Phys.* **13** 931
- [20] Johnson R D et al 2015 *Phys. Rev. B* **92** 235119
- [21] Ziatdinov M et al 2016 *Nat. Commun.* **7** 13774
- [22] Cao H B, Banerjee A, Yan J-Q, Bridges C A, Lumsden M D, Mandrus D G, Tennant D A, Chakoumakos B C and Nagler S E 2016 *Phys. Rev. B* **93** 134423
- [23] Supplementary material
- [24] Kitaev A 2006 *Ann. Phys.* **321** 2
- [25] Baskaran G, Mandal S and Shankar R 2007 *Phys. Rev. Lett.* **98** 247201
- [26] Knolle J, Kovrizhin D L, Chalker J T and Moessner R 2014 *Phys. Rev. Lett.* **112** 207203
- [27] Knolle J, Chern G, Kovrizhin D L, Moessner R and Perkins N B 2014 *Phys. Rev. Lett.* **113** 187201
- [28] Sandilands L J, Tian Y, Plumb K W, Kim Y-J and Burch K S 2015 *Phys. Rev. Lett.* **114** 147201
- [29] Nasu J, Knolle J, Kovrizhin D L, Motome Y and Moessner R 2016 *Nat. Phys.* **12** 912
- [30] Banerjee A et al 2016 *Nat. Mater.* **15** 733
- [31] Ran K et al 2017 *Phys. Rev. Lett.* **118** 107203
- [32] Do S-H et al 2017 *Nat. Phys.* **13** 1079
- [33] Banerjee A et al 2018 *NPJ Quantum Mater.* **3** 8
- [34] Winter S M, Riedl K, Maksimov P A, Chernyshev A L, Honecker A and Valent R 2017 *Nat. Commun.* **8** 1152
- [35] Kasahara Y et al 2018 *Nature* **559** 227
- [36] Kuzmenko A B 2005 *Rev. Sci. Instrum.* **76** 083108
- [37] Kuzmenko A B 2017 Reffit v. 1.3.03, University of Geneva (<https://sites.google.com/site/refitprogram/>)
- [38] Hasegawa Y, Aoyama T, Sasaki K, Ikemoto Y, Moriwaki T, Shirakura T, Saito R, Imai Y and Ohgushi K 2017 *J. Phys. Soc. Japan* **86** 123709
- [39] Biesner T et al 2018 *Phys. Rev. B* **97** 220401
- [40] Guizzetti G, Reguzzoni E and Pollini I 1979 *Phys. Lett. A* **70** 34
- [41] Little A et al 2017 *Phys. Rev. Lett.* **119** 227201
- [42] Emeis C A, Reinders F J and Drent E 1975 *Solid State Commun.* **16** 239
- [43] Bermudez V M 1976 *Solid State Commun.* **19** 693
- [44] Borghesi A, Guizzetti G, Marabelli F, Nosenzo L and Reguzzoni E 1984 *Solid State Commun.* **52** 463
- [45] Wolter A U B et al 2017 *Phys. Rev. B* **96** 041405
- [46] Kanesaka I, Kawahara H, Yamazaki A and Kawai K 1986 *J. Mol. Struct.* **146** 41
- [47] Yadav R, Bogdanov N A, Katukuri V M, Nishimoto S, van den Brink J and Hozoi L 2016 *Sci. Rep.* **6** 37925
- [48] Sandilands L J, Sohn C H, Park H J, Kim S Y, Kim K W, Sears J A, Kim Y-J and Noh T W 2016 *Phys. Rev. B* **94** 195156
- [49] Sandilands L J, Tian Y, Reijnders A A, Kim H-S, Plumb K W, Kim Y-J, Kee H-Y and Burch K S 2016 *Phys. Rev. B* **93** 075144
- [50] Binotto L, Pollini I and Spinolo G 1971 *Phys. Status Solidi b* **44** 245
- [51] Sinn S et al 2016 *Sci. Rep.* **6** 39544
- [52] Geschwind S and Remeika J P 1962 *J. Appl. Phys.* **33** 370
- [53] Mittelstädt L, Schmidt M, Wang Zhe, Mayr F, Tsurkan V, Lunkenheimer P, Ish D, Balents L, Deisenhofer J and Loidl A 2015 *Phys. Rev. B* **91** 125112
- [54] Laurita N J, Deisenhofer J, Pan L, Morris C M, Schmidt M, Johnsson M, Tsurkan V, Loidl A and Armitage N P 2015 *Phys. Rev. Lett.* **114** 207201
- [55] Reschke S, Wang Z, Mayr F, Ruff E, Lunkenheimer P, Tsurkan V and Loidl A 2017 *Phys. Rev. B* **96** 144418
- [56] Warren M T, Pokharel G, Christianson A D, Mandrus D and Valdés Aguilar R 2017 *Phys. Rev. B* **96** 054432
- [57] Bolens A, Katsura H, Ogata M and Miyashita S 2018 *Phys. Rev. B* **97** 161108
- [58] Aoyama T, Hasegawa Y, Kimura S, Kimura T and Ohgushi K 2017 *Phys. Rev. B* **95** 245104
- [59] Shi L Y, Liu Y Q, Lin T, Zhang M Y, Zhang S J, Wang L, Shi Y G, Dong T and Wang N L 2018 *Phys. Rev. B* **98** 094414
- [60] Wu L et al 2018 *Phys. Rev. B* **98** 094425
- [61] Banerjee A, Yan J, Knolle J, Bridges C A, Stone M B, Lumsden M D, Mandrus D G, Tennant D A, Moessner R and Nagler S E 2017 *Science* **356** 1055
- [62] Agrestini S et al 2017 *Phys. Rev. B* **96** 161107
- [63] Wang W, Dong Z-Y, Yu S-L and Li J-X 2017 *Phys. Rev. B* **96** 115103
- [64] Gretarsson H et al 2013 *Phys. Rev. Lett.* **110** 076402